

Review

Application of Zr and Ti-Based Bulk Metallic Glasses for Orthopaedic and Dental Device Materials

Kazuhiro Imai * , Xiao Zhou and Xiaoxuan Liu

Department of Life Sciences, Graduate School of Arts and Sciences, The University of Tokyo, Tokyo 153-8902, Japan; syuusyou1988@yahoo.co.jp (X.Z.); luluxxliu@gmail.com (X.L.)

* Correspondence: imai@idaten.c.u-tokyo.ac.jp; Tel.: +81-3-5454-6133

Received: 1 January 2020; Accepted: 29 January 2020; Published: 1 February 2020



Abstract: Conventional orthopaedic and dental device materials are made of metallic materials such as stainless steel (SUS316L), titanium alloy (Ti-6Al-4V), and cobalt-chrome (Co-Cr). Those materials have the disadvantage of mechanical properties and anti-corrosion behavior. Bulk metallic glasses (BMGs), which are also called amorphous alloys, are metallic materials with metastable glassy states and have a higher strength, higher elasticity, higher failure resistance, and lower Young's modulus compared with crystalline alloys. There are several types of BMGs. Among them, Zr-based BMGs and Ti-based BMGs have excellent mechanical properties. In addition, they have good corrosion resistance and are promising for orthopaedic and dental device materials. In this review article, *in vitro* and *in vivo* studies regarding Zr and Ti-based BMGs applications as biomaterials, especially in orthopaedic and dental device materials, are reviewed.

Keywords: amorphous alloy; bulk metallic glasses; orthopaedic device; dental device; implant; anti-corrosion; biocompatibility

1. Introduction

Biomaterials are materials that are used for therapy and interact with biological systems. They are often used and adapted for medical and dental applications, and are in contact with body fluids, tissues, and cells. In case of organ or tissue damage, degeneration, or dysfunction, biomaterials are used as functional replacements. There are many device materials in which biomaterials are used, i.e., joint replacements, bone fixation devices, tooth fixation implants, blood vessel prostheses, and heart valves. Those device materials need to be non-toxic, anti-corrosion, strong, and tough because they are continuously receiving a reaction from biological systems and bearing daily loadings. In those conditions, metals as well as polymers or ceramics are used as biomaterials. Metals including stainless steel (SUS316L), titanium alloy (Ti-6Al-4V), and cobalt-chrome (Co-Cr) have the advantages of strength, toughness, and elasticity and are used in joint replacements, bone fixation devices, tooth implants, and heart pacemakers. Ceramics, including alumina, zirconia, and hydroxyapatite, have the advantages of strength and anti-abrasion and are used in joint replacements and tooth implants. Polymers, including polymethylmethacrylate (PMMA), silicone, and polyurethanes, have the advantages of workability and are lightweight. These polymers are used in catheters, vascular grafts, and intraocular lenses.

Some types of biomaterials have been made and applied as implanted device materials in medical and dental practice. Especially in orthopaedic fields, load bearing is essential and metallic materials mainly consist of SUS316L, Ti-6Al-4V, and Co-Cr, which are widely used because metals have high mechanical strength. However, there are several limitations when metallic implants are used for orthopaedic and dental device materials. When biomaterials are implanted into patients for bone fracture repairs, they are loaded repeatedly in daily activities. In addition, implanted biomaterials are in direct contact with body fluids and tissues. In those conditions, the implants are sometimes failed

or broken by fretting corrosion fatigue [1,2]. To prevent failure or breakage, the devices or implants, such as bone plates or nails, have been made bulky enough. During surgery, long incision is needed to implant a bone plate. After the implantation, closing the skin wound is sometimes difficult. Likewise, to prevent nail failure, an intramedullary nail needs to have a large diameter. Such nails with a large diameter occupy a large area of the medullary canal and block the blood supply, which may incur fracture healing delay. In this way, strength deficiency of the conventional metallic devices is one of the disadvantages and limitations. Another limitation is that Young's moduli of conventional metallic devices are too high. Those metallic devices have the Young's modulus of 100–110 GPa, which is much higher than cortical bone of 15–20 GPa. Stress shielding occurs from the Young's modulus discrepancy between the osteo-synthetic device made of these materials and human bone, and sometimes leads to absorption of the bone around the material [3–7]. Regarding dental root implants, pure Ti and Ti-6Al-4V are universally used, but shielding effect is incurred by significant Young's modulus discrepancy between the Ti alloy and human bone. The stress shielding effect because of the implant's high Young's modulus has been shown as one of the major reasons of implant failure. In addition, SUS316L and Co-Cr release the toxic elements, such as Ni, Cr, and Co. Titanium alloys including Ti-6Al-4V have the disadvantage of low hardness and sometimes suffer from poor wear resistance.

Bulk metallic glasses (BMGs), which are also called amorphous alloys, are another type of metallic materials with metastable glassy states. Most metals are crystalline, which have an atomic structure with a highly ordered arrangement. On the other hand, BMGs have a glass-like structure and a state of non-crystalline. BMGs are prepared by extremely rapid cooling and solidification of melting liquid alloys. The speed of cooling and solidification is high enough. Therefore, the nucleation of crystals can be suppressed without a long-range atomic order. Due to their amorphous atomic structures, BMGs show unique mechanical, physical, and chemical properties and are superior to conventional metallic alloys, i.e., crystalline alloys. On the other hand, the crystalline alloy has grain boundaries, dislocations, and segregations, which are disadvantageous. When the crystalline alloy is subjected to loading, it can easily fail because of its grain boundaries and dislocations. The crystalline alloy has slip planes. Shear stress can move the atomic structure alongside the slip plane and lead to plastic deformation. The plastic deformation can also be enhanced by the dislocations.

In contrast, BMGs have a random and disordered atomic structure without segregations. In BMGs, there are no slip planes generated, and mass movement of the constituent atoms causes elastic deformation until it is under high stresses (Figure 1). As such, BMGs have higher strength, higher elasticity, higher failure resistance, and lower Young's modulus compared to crystalline alloys. With the combination of unique mechanical, physical, and chemical properties, BMGs have a wide range of potential applications including using biomaterials. In this review article, studies regarding Zr-based and Ti-based BMGs applications as biomaterials, especially in orthopaedic and dental device materials, are reviewed.

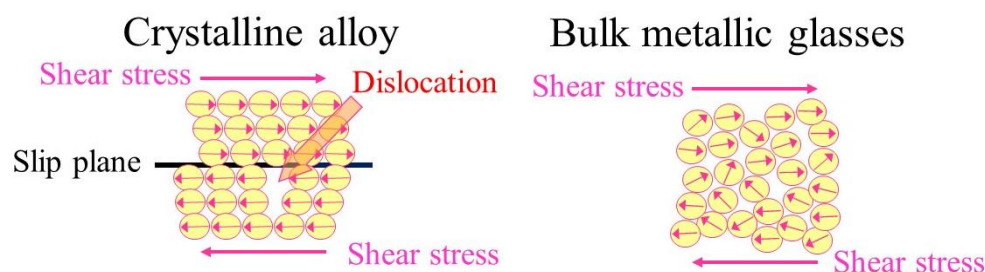


Figure 1. Atomic structures of crystalline alloy and bulk metallic glasses (BMGs). With shear stress, dislocation in a crystalline alloy causes plastic transformation. In BMGs, movement of the mass of atoms induces elastic transformation.

2. Classification of BMGs

BMGs with an amorphous atomic structure is formed as an alloy rather than a pure metal. Three basic rules to form BMGs have been reported [8]. The BMGs alloy constituent materials are made of at least three components. The components' atomic radiuses have to be significantly different to achieve low free volume and high packing density. Among the main constituent materials, the atomic radius of each other should have more than a 12% difference. Based on these basic rules of choosing the appropriate compositions, Mg, Ca, Sr, lanthanide metal (Ln), Ti, Zr, Hf, Fe, Co, Ni, Pd, Pt, Cu, and Au-based BMGs have been produced. Samples with more than 20 mm diameters have been produced based on Mg, Ln, Zr, Fe, Ni, Pd, Pt, and Cu-based BMGs [9–16].

The BMGs are classified into seven groups based on the main component, atomic size difference, and constituent elements [17], and G-I to G-VII (Table 1). Each group has several alloys. The representative of G-I is Zr-Al-Ni-Cu, G-II is Co-Fe-Ta-B, G-III is Fe-Al-Ga-P-C-B, G-IV is Zr-Ti-Be-Ni-Cu, G-V is Pd-Cu-Ni-P, G-VI is Ti-Zr-Cu-Ni, and G-VII is Ca-Mg-Cu, respectively. The radius of the main atom is the smallest in G-VI. In G-II and G-IV, the atomic radius of the main element is intermediate, and it is the largest in G-I, G-V, and G-VII. Properties of BMGs are dependent on the main constituent. The BMGs showed excellent corrosion resistance, high tensile strength, high elastic energy, high impact fracture energy, and excellent ductility for Zr-based BMGs [18] and good soft magnetic properties with high saturation magnetization and low coercivity for Fe-based and Co-based BMGs [19].

Table 1. Classification of bulk metallic glasses (BMGs).

Group	Representatives
I	Zr-Al-Ni, Zr-Al-Cu, Ln-Al-Ni, Ln-Al-Cu Zr-Al-Ni-Cu, Ln-Al-Ni-Cu, Zr-Ti-Al-Ni-Cu Zr-Ga-Ni, Ln-Ga-Ni, Ln-Ga-Cu
II	Fe-Zr-B, Fe-Hf-B Fe-Zr-Hf-B, Fe-Co-Ln-B Co-Zr-Nb-B, Co-Fe-Ta-B
III	Fe-(Al, Ga)-Metalloid
IV	Mg-Ln-Ni, Mg-Ln-Cu Zr-Ti-Be-Ni-Cu, Ti-Cu-Ni-Sn-Be, Ti-Cu-Ni-Sn-Be-Zr
V	Pd-Ni-P, Pd-Cu-Ni-P, Pt-Ni-P
VI	Cu-Zr-Ti, Ni-Nb-Ta, Ni-Nb-Sn Ti-Zr-Cu-Ni, Ti-Ni-Cu-Sn, Ti-Cu-Ni-Mo-Fe
VII	Ca-Mg-Cu, Ca-Mg-Zn

3. Mechanical Properties of Zr and Ti-Based BMGs

Zr-based BMGs have excellent corrosion resistance and wear resistance, high tensile strength, high elastic energy, and relatively low Young's modulus [20–23]. The ultimate tensile strengths of Zr-based BMGs are 1500–1700 MPa, which is approximately twice that of Ti-6Al-4V alloy and three times that of SUS316L [18,24–27]. The Young's moduli of Zr-based BMGs are 70–80 GPa, and are closer to Young's modulus of bone than conventional materials [28–31]. Zr-based BMGs show the fatigue strengths ranging from 560 to 980 MPa and the yield strengths ranging from 1500 to 1900 MPa [32]. The fatigue behavior was affected by the fabrication process, Poisson's ratio, and surface condition [33,34]. Mechanical properties, corrosion resistance, and cytotoxicity of Ni-free Zr-based BMGs were examined [35–37]. The ultimate compression strengths of $Zr_{60}Nb_5Cu_{22.5}Pd_5Al_{7.5}$ BMGs and $Zr_{60}Nb_5Cu_{20}Fe_5Al_{10}$ BMGs were 1724 and 1795 MPa, respectively. The Young's moduli of the BMGs were 70–85 GPa, and closer to Young's modulus of bone than conventional materials [35]. Yield strengths of $Zr_{50}Cu_{35}Al_7Nb_5Pd_3$ BMGs and $Zr_{55}Cu_{30}Al_7Nb_5Pd_3$ BMGs were 1806 and 1664 MPa,

respectively. The Young's moduli of them were 88 and 86 GPa, respectively. The Zr-Cu-Al-Nb-Pd BMGs exhibited high Vickers hardness values (HV) above 4700 MPa [36]. $Zr_{60.14}Cu_{22.31}Fe_{4.85}Al_{9.7}Ag_3$ BMGs, sample rods of 2 mm diameter, also showed high fracture tensile strength of 1720 MPa, a relative low Young's modulus of 82 GPa, and high hardness values of 4200 MPa [37].

Mechanical properties of 316L stainless steel, Ti-6Al-4V alloy, Zr-based BMGs, and human bone are summarized in Table 2.

Table 2. Mechanical properties of 316L stainless steel, Ti-6Al-4V alloy, Zr-based bulk metallic glasses (BMGs), and human bone.

Mechanical Properties	Yield Strength (MPa)	Fracture Strength (MPa)	Young's Modulus (GPa)	Hardness (MPa)
316L stainless steel [25–27]	>175	190–690	200–203	3580
Ti-6Al-4V alloy [24,26,27]	853	950	108–116	3138
$Zr_{65}Al_{7.5}Ni_{10}Cu_{17.5}$ BMGs [18]	-	1500–1700	70–80	-
$Zr_{60}Nb_5Cu_{22.5}Pd_5Al_{7.5}$ BMGs [35]	1378	1724	70–85	-
$Zr_{60}Nb_5Cu_{20}Fe_5Al_{10}$ BMGs [35]	1393	1795	70–85	-
$Zr_{50}Cu_{35}Al_7Nb_5Pd_3$ BMGs [36]	1806	-	88	5060
$Zr_{55}Cu_{30}Al_7Nb_5Pd_3$ BMGs [36]	1664	-	86	4790
$Zr_{60.14}Cu_{22.31}Fe_{4.85}Al_{9.7}Ag_3$ BMGs [37]	-	1720	82	4200
Human bone (femur) [28–31]	80	120	15–20	-

Ti-based BMGs also have superior mechanical properties compared to crystalline Ti alloys (Table 3). The yield strengths of Ti-based BMGs are 2000 ± 78 MPa, which is approximately 2.5 times as much as the yield strength of pure titanium and Ti-6Al-4V alloy. The Young's moduli of Ti-based BMGs are 80 ± 12 GPa, and are closer to Young's modulus of bone than conventional biomaterials [38].

Table 3. Mechanical properties comparison of Ti-based BMGs, conventional biomaterials, and human bone.

Mechanical Properties	Yield Strength (MPa)	Young's Modulus (GPa)
316L stainless steel	>175	200–203
Ti-6Al-4V alloy	853	108–116
Pure titanium	800 ± 50	100 ± 7
Ti-based BMGs	2000 ± 78	80 ± 12
Human bone (femur)	80	15–20

4. In Vitro Studies for Biomaterial Applications

4.1. Zr-Based BMGs

Due to the properties with excellent corrosion resistance, high strength, high fatigue limit, and relative low modulus, Zr-based BMGs are promising for biomaterial applications. As *in vitro* experiments, $Zr_{65}Al_{7.5}Ni_{10}Cu_{17.5}$ BMGs in a phosphate buffered solution (PBS) were investigated to assess the effect of chloride-ion concentration and dissolved oxygen pressure on the polarization behavior. Zr-based BMGs showed high anti-corrosion performance in physiological environments [39–44]. To show biocompatibility, the electrochemical interactions, which result in the release of metal ions into the surrounding tissue, have been evaluated. Electrochemical characterization was performed at 37 °C in PBS electrolyte simulating conditions similar to *in vivo* [45]. Electrochemical cyclic-anodic-polarization tests were conducted and the corrosion penetration rate (CPR) values were estimated for $Zr_{52.5}Cu_{17.9}Ni_{14.6}Al_{10.0}Ti_{5.0}$ BMG, SUS316L, Co-Cr-Mo alloy, and Ti-6Al-4V [46]. The mean ($\pm 95\%$ CIs) CPR values of $Zr_{52.5}Cu_{17.9}Ni_{14.6}Al_{10.0}Ti_{5.0}$ BMGs was 0.8 ± 0.4 $\mu\text{m}/\text{year}$, and significantly lower than the mean CPR values of SUS316L, which was 1.5 ± 0.4 $\mu\text{m}/\text{year}$. The result indicated that $Zr_{52.5}Cu_{17.9}Ni_{14.6}Al_{10.0}Ti_{5.0}$ BMGs demonstrated better corrosion resistance compared

to SUS316L. However, CPR values of the Co-Cr-Mo alloy and Ti-6Al-4V were much lower (Co-Cr-Mo alloy, $0.3 \pm 0.2 \mu\text{m/year}$, Ti-6Al-4V; $0.3 \pm 0.2 \mu\text{m/year}$) and showed better corrosion resistance [45].

In vitro biocompatibility of $\text{Zr}_{41}\text{Ti}_{14}\text{Cu}_{12}\text{Ni}_{10}\text{Be}_{23}$ BMGs, $\text{Zr}_{44}\text{Ti}_{11}\text{Cu}_{10}\text{Ni}_{10}\text{Be}_{25}$ BMGs, and $\text{Zr}_{57}\text{Nb}_5\text{Cu}_{15.4}\text{Ni}_{12.6}\text{Al}_{10}$ BMGs were investigated by *in vitro* corrosion resistance evaluation and cytotoxicity evaluation with pure Ti and pure Zr as controls [47]. The BMGs were immersed in pH 7.4 simulated body fluid (SBF) and pH 6.3 artificial saliva (AS). As the result, all the immersed BMGs samples had better anti-corrosion properties in AS than in SBF, and corrosion resistance of $\text{Zr}_{44}\text{Ti}_{11}\text{Cu}_{10}\text{Ni}_{10}\text{Be}_{25}$ BMGs was comparable with pure Ti and pure Zr. The pitting corrosion potentials of $\text{Zr}_{44}\text{Ti}_{11}\text{Cu}_{10}\text{Ni}_{10}\text{Be}_{25}$ BMGs were much higher than that of pure Zr. The experiment to assess direct cytotoxicity showed that cells could adhere well on the Zr-based BMGs sample surface [47]. Most Zr-based BMGs contain Ni, which is commonly blamed of possible allergy occurrence and a possible carcinogenic factor for the human [48]. Therefore, Ni-free Zr-based BMGs might be more appropriate for biomaterial use.

Zr-based BMGs' corrosion behaviors in phosphate buffered solution were evaluated by electrochemical polarization and the excellent corrosion resistance was revealed [35–37]. The excellent corrosion resistance might come from the passive film formation on the surface. X-ray photoelectron spectroscopy (XPS) was used to assess the chemical compositions on the surface, and the oxide film formed on the surface of the Zr-based BMGs. The oxide film that consisted of ZrO_2 , Al_2O_3 , and Nb_2O_5 were observed [36,37]. The results indicated that the enriched oxides on the Zr-based BMGs surface might provide excellent anti-corrosion performance and prevention of corrosive reactions in phosphate buffered solution.

The Zr-based BMGs cytotoxicity evaluation by a one-week cell culture showed a good biocompatibility as Ti-6Al-4V [18,35]. Cell adhesions and morphologies after four hours of incubation showed the biocompatibility and biosafety [36]. Ni-free Zr-based BMGs showed good biocompatibility and biocorrosion *in vitro* study [49,50]. Powder consolidated $\text{Zr}_{76.6}\text{Al}_{3.5}\text{Ni}_{7.6}\text{Cu}_{12.3}$ BMGs, which showed fatigue strength equivalent to that of pure Ti [26]. An *in vitro* biocompatibility assessment of $\text{Zr}_{61}\text{Ti}_2\text{Cu}_{25}\text{Al}_{12}$ BMGs and cylindrical rods 6 mm in diameter for a potential application in dental implants showed that the in-cellular response for $\text{Zr}_{61}\text{Ti}_2\text{Cu}_{25}\text{Al}_{12}$ BMGs biocompatibility was comparable to Ti and Ti alloys [51]. The good biocompatibility and good corrosion-resistance in the physiological environment of $\text{Zr}_{61}\text{Ti}_2\text{Cu}_{25}\text{Al}_{12}$ BMGs was associated with the zirconium oxide layer formation on the surface.

4.2. Ti-Based BMGs

Rod-shaped $\text{Ti}_{40}\text{Zr}_{10}\text{Cu}_{38}\text{Pd}_{12}$ BMGs, which are 2.5 mm in diameter, showed a hardness value of 9400 MPa, which was much larger than that of the Ti-6Al-4V alloy of 3138 MPa [52]. *In vitro* test in Hank's solution of the $\text{Ti}_{40}\text{Zr}_{10}\text{Cu}_{38}\text{Pd}_{12}$ BMGs rod showed anti-corrosion performance as good as Ti-6Al-4V alloy. The performance of the $\text{Ti}_{40}\text{Zr}_{10}\text{Cu}_{38}\text{Pd}_{12}$ BMGs rod in the anodic region suggested the existence of wide passive regions, which were related to protective passive film formation. The mechanism of the high anti-corrosion performance of Ti-based BMGs was connected to the rapid formation of protective oxide films, mainly TiO_2 , which were stable, continuous, and highly adherent on metal surfaces in a wide range of the corrosive region.

In vitro biocompatibility assessment of $\text{Ti}_{40}\text{Cu}_{38}\text{Zr}_{10}\text{Pd}_{12}$ BMGs, 3 mm in diameter for a potential application in orthopaedic implants, showed differentiation into osteoblasts and Cu ion release [53]. The low levels of inflammatory cytokines secretion showed the absence of an immunogenic response to the $\text{Ti}_{40}\text{Cu}_{38}\text{Zr}_{10}\text{Pd}_{12}$ BMGs. The biocompatibility assessment suggested that the $\text{Ti}_{40}\text{Cu}_{38}\text{Zr}_{10}\text{Pd}_{12}$ BMGs rod allow pre-osteoblasts to adhere to a mirror-like surface and to differentiate into osteoblasts under the appropriate culture conditions, which prevented the inflammatory response.

In vitro anti-corrosion and cytotoxicity assessment of $\text{Ti}_{41.5}\text{Zr}_{2.5}\text{Hf}_5\text{Cu}_{37.5}\text{Ni}_{7.5}\text{Si}_1\text{Sn}_5$ BMGs was investigated, with cylindrical rods 3 mm in diameter and a mirror-like surface for potential application in dental implants [54]. $\text{Ti}_{41.5}\text{Zr}_{2.5}\text{Hf}_5\text{Cu}_{37.5}\text{Ni}_{7.5}\text{Si}_1\text{Sn}_5$ BMGs showed great corrosion resistance in

electrochemical measurements due to the oxide film that formed on its surface. Regarding pitting corrosion, anti-corrosion properties in artificial saliva (AS) solution were much higher than those in SBF solution. The cytotoxicity results showed that $\text{Ti}_{41.5}\text{Zr}_{2.5}\text{Hf}_5\text{Cu}_{37.5}\text{Ni}_{7.5}\text{Si}_1\text{Sn}_5$ BMGs had low cell viability on murine fibroblast cells. The BMGs have better anti-corrosion properties because of the lack of grain boundaries. In addition, $\text{Ti}_{41.5}\text{Zr}_{2.5}\text{Hf}_5\text{Cu}_{37.5}\text{Ni}_{7.5}\text{Si}_1\text{Sn}_5$ BMGs has a stable surface in the same level of pure Ti, which was attributed to the oxide film formed on the surface. As a promising dental implant material, $\text{Ti}_{41.5}\text{Zr}_{2.5}\text{Hf}_5\text{Cu}_{37.5}\text{Ni}_{7.5}\text{Si}_1\text{Sn}_5$ BMGs was found safe in the human body [54].

5. In Vivo Studies for Biomaterial Applications

Compared to abundant *in vitro* studies for BMGs biomedical applications, *in vivo* animal tests of BMGs are currently limited. However, the results of *in vivo* studies have shown that Zr-based BMGs and Ti-based BMGs are promising materials for orthopaedic and dental applications. All the animal tests were approved by the ethics committee of the institute based on the *in vitro* studies to prove the safety, anti-corrosion, and non-cytotoxicity of BMGs.

5.1. Animal Tests of Zr-Based BMGs

There are three types of Zr-based BMGs animal tests. The first type is the intramedullary nails in rat femora [55]. $\text{Zr}_{65}\text{Al}_{7.5}\text{Ni}_{10}\text{Cu}_{17.5}$ BMGs rods 2 mm in diameter and 40 mm in length were implanted as osteosynthesis intramedullary nails in rat femora after osteotomy (Figure 2). After 12 weeks implantation, systemic effects were investigated using the blood test. Local effects were investigated using graphite furnace atomic absorption spectroscopy. Removed implants were investigated using scanning electron microscopy (SEM) and energy dispersion X-ray spectroscopy (EDS). Osteotomy healings were investigated and compare $\text{Zr}_{65}\text{Al}_{7.5}\text{Ni}_{10}\text{Cu}_{17.5}$ BMGs with Ti-6Al-4V alloy using mechanical testing and peripheral quantitative computed tomography (pQCT) evaluation. From the results of systemic effects and local effects, there were no harmful effects after 12 weeks of implantation. The SEM (Figure 3) and EDS (Figure 4) results of the removed implants indicated that $\text{Zr}_{65}\text{Al}_{7.5}\text{Ni}_{10}\text{Cu}_{17.5}$ BMGs were almost biologically inert. The results of mechanical testing and pQCT evaluation indicated that $\text{Zr}_{65}\text{Al}_{7.5}\text{Ni}_{10}\text{Cu}_{17.5}$ BMGs had the tendency to get better osteotomy healing than the Ti-6Al-4V alloy even though the difference did not reach significance.

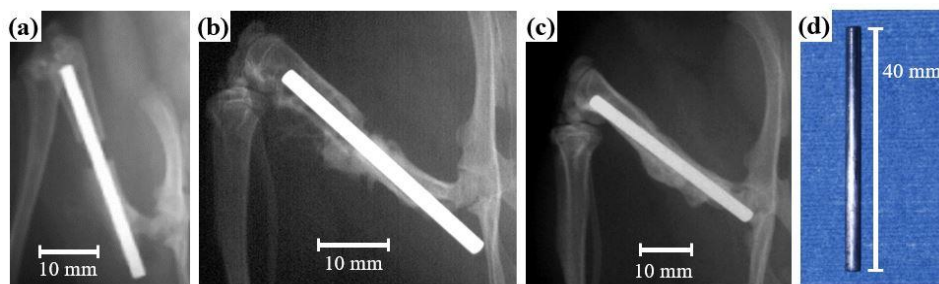


Figure 2. $\text{Zr}_{65}\text{Al}_{7.5}\text{Ni}_{10}\text{Cu}_{17.5}$ bulk metallic glasses (BMGs) rod implantation in rat femora after osteotomy as an intramedullary nail. (a) X-ray image of femoral bone immediately after osteotomy and BMGs intramedullary nail implantation. (b) X-ray image after implantation for six weeks. (c) X-ray image after implantation for 12 weeks. (d) Removed $\text{Zr}_{65}\text{Al}_{7.5}\text{Ni}_{10}\text{Cu}_{17.5}$ BMGs rod after 12 weeks of implantation.

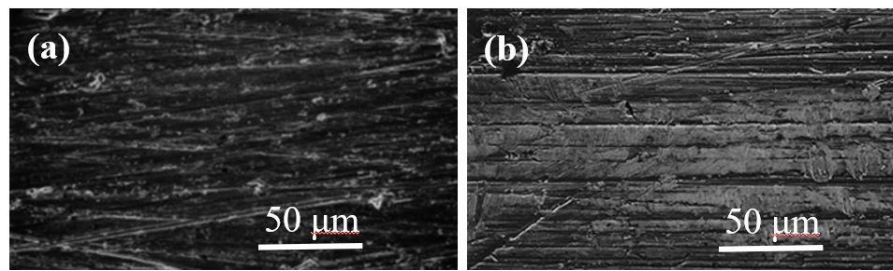


Figure 3. Scanning electron microscopy (SEM) images of $Zr_{65}Al_{7.5}Ni_{10}Cu_{17.5}$ BMGs rod (a) before and (b) after 12 weeks of implantation. Polishing scars were observed in both images. No reactions nor changes were observed after the *in vivo* experiment.

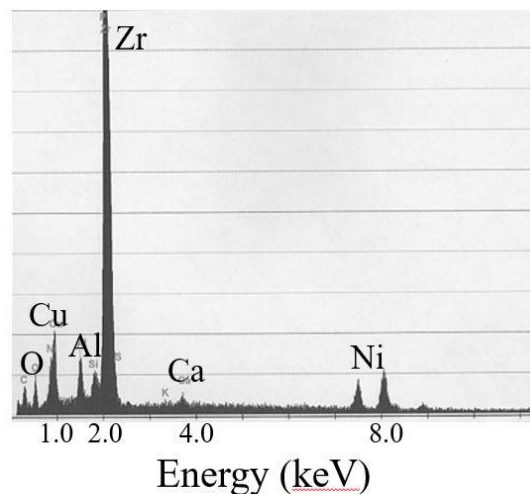


Figure 4. Energy dispersion X-ray spectroscopy (EDS) image of $Zr_{65}Al_{7.5}Ni_{10}Cu_{17.5}$ BMGs rod after 12 weeks of implantation. Oxygen (O) and calcium (Ca) were noted with the exception of Zr, Al, Ni, Cu. No element of corrosion was noted, which showed anti-corrosion behaviour.

The second type is the embedded samples in the rabbit femora [56]. Zr-Cu-Al-Ag BMGs cylindrical rods 2 mm in diameter and 6 mm in length were implanted to evaluate the *in vivo* biocompatibility. After four weeks, eight weeks, and 12 weeks of implantation, removed implants were observed via SEM equipped with EDS. Tissues around the implant were investigated through a histological examination. After eight weeks and 12 weeks of implantation, no gap could be observed between the bone tissue and implant samples, which indicated that Zr-Cu-Al-Ag BMGs exhibits new bone formation and excellent *in vivo* biocompatibility. There were no inflammatory reactions or osteonecrosis changes.

The third type is the sub-periosteal implanted on the bone surface of rat femora [57,58]. $Zr_{65}Al_{7.5}Ni_{10}Cu_{17.5}$ BMGs ribbons 10 mm in length, 2 mm in width, and 0.5 mm in thickness were implanted on the bone surface for six weeks (Figure 5). After the implantation, systemic effects were investigated using a blood test. Femur and soft tissues around the implant were investigated through a histological examination. Removed implants were investigated using SEM equipped with EDS. The results show that blood levels of Cu and Ni did not increase, and no findings of the biological effects were recognized including cell necrosis or dysplasia, infiltration of inflammatory cells, bone resorption, and wear debris of the alloy. Regarding removed implants, there were no findings of breakage nor pitting corrosion.

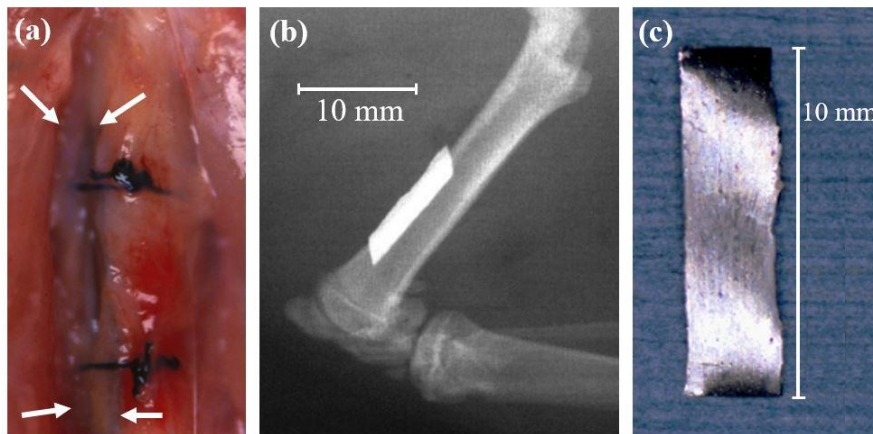


Figure 5. $Zr_{65}Al_{7.5}Ni_{10}Cu_{17.5}$ BMGs ribbon sub-periosteal implantation on the bone surface of rat femoral bone. (a) BMGs ribbon (arrows) was implanted and tied to the femoral bone with 4-0 nylon suture string. (b) The X-ray image after implantation for six weeks. (c) Removed $Zr_{65}Al_{7.5}Ni_{10}Cu_{17.5}$ BMGs ribbon after six weeks of implantation.

Among the three types of Zr-based BMGs *in vivo* animal tests, there were no sign of systemic effects, local inflammatory reactions or osteonecrosis changes, and breakage or pitting corrosion of the implants. The first study and the second study revealed that Zr-based BMGs had good biocompatibility. The first study showed the Zr-based BMGs implant as an osteosynthesis device. Osteotomy healing occurred as fast as the Ti-6Al-4V alloy. The first and the third study concluded that Zr-based BMGs implants were nearly biologically inert and were promising for eventually removed osteosynthesis devices. On the other hand, the second study concluded that the Zr-based BMGs implant shows excellent new bone formation around the implant, which might be suitable for osteosynthesis devices that are implanted eternally. Zr-based BMGs implants are promising, especially in orthopaedic and dental device materials, but further investigation will be needed to know whether Zr-based BMGs implants should be implanted temporally or eternally.

5.2. Animal Tests of Ti-Based BMGs

There are three types of Ti-based BMG animal tests. The first type is the dental material in beagle dog's mandible [54]. $Ti_{41.5}Zr_{2.5}Hf_5Cu_{37.5}Ni_{7.5}Si_1Sn_5$ BMGs samples 3 mm in diameter and 5 mm in length were implanted in one side of the beagle dogs' mandible for one month. There was no inflammation observed around the BMGs sample. The histological examination and EDS analysis showed that the $Ti_{41.5}Zr_{2.5}Hf_5Cu_{37.5}Ni_{7.5}Si_1Sn_5$ BMGs samples are well integrated with the bone tissue and new bone was formed around the samples, which proved the *in vivo* biocompatibility [54].

The second type is the $Ti_{40}Zr_{10}Cu_{34}Pd_{14}Sn_2$ BMGs alloy bar in rat femora implanted for three months [59]. The Ti-based BMGs sample showed good compatibility with bone integration ability, and no component material ion diffusion, which indicated that the Ti-based BMGs is promising for bone implants.

The third type is the implanted material in the cavity of rat tibial tubercle [60]. $Ti_{45}Zr_{40}Si_{15}$, $Ti_{40}Zr_{40}Si_{15}Cu_5$, and $Ti_{45}Zr_{20}Cu_{35}$ BMGs ribbons with 6 mm in length, 3 mm in width, and 1.0–1.5 mm in thickness were implanted for 3, 6, and 12 weeks. There were no findings of septic or inflammatory reactions. The X-ray photographs showed that the thin callus layer and woven bone were formed directly on the BMGs ribbons, which explained good biocompatibility. The SEM images of $Ti_{45}Zr_{20}Cu_{35}$ BMGs ribbons showed the presence of significant small cavities in the cortical tibial bone. The sample implanted with $Ti_{45}Zr_{40}Si_{15}$ BMGs ribbons had a high cortical bone density. Therefore, Cu-free $Ti_{45}Zr_{40}Si_{15}$ BMGs has good potential for biomaterials in orthopaedic and dental device materials.

5.3. Animal Tests of Mg-Based, Sr-Substituted, and Nanopatterned Pt-Based BMGs

Besides Zr and Ti-based BMGs that are non-biodegradable, there are Mg, Zn, Ca, and Sr-based BMGs, which are biodegradable. Biodegradable materials are useful to apply as orthopaedic materials such as absorbable screws and artificial bones. However, biodegradable materials inevitably cause reactions between the implants and the tissues. Therefore, biocompatibility of biodegradable BMGs should be evaluated by *in vivo* animal tests.

Mg₆₀Zn₃₅Ca₅ BMGs were implanted in rabbit femur as a tendon-bone interference fixation model for 24 weeks [61] compared to the Ti-6Al-4V alloy and polylactic acid (PLA). After 24 weeks of implantation, no inflammatory cells such as leukocytes or macrophages were observed in all of Mg₆₀Zn₃₅Ca₅ BMGs, Ti-6Al-4V alloy, and PLA, which indicates the good biocompatibility of Mg₆₀Zn₃₅Ca₅ BMGs. Micro-CT images and histology observation showed new bone formation surrounding the Mg₆₀Zn₃₅Ca₅ BMGs and the Ti-6Al-4V alloy. In addition, more sustainable osteo-promoting effects were found in Mg₆₀Zn₃₅Ca₅ BMGs when compared to the Ti-6Al-4V alloy after 24 weeks of implantation.

Strontium-substituted SiO₂-Al₂O₃-P₂O₅-CaO-CaF₂ BMGs were implanted in bone defects of rabbit femur for 26 weeks [62]. There was no finding of an adverse effect including inflammation or necrosis. There was some evidence of good bone regeneration and a remodeling process in bone defects. Newly formed bone is integrated between Strontium-substituted BMGs and the host bone. These findings indicated the good biocompatibility of Strontium-substituted BMGs and the possibility of application as artificial bone or a bioactive implant-like hydroxyapatite (HA) implant.

Nanopatterned Pt-based BMGs biomaterials were implanted subcutaneously in mice for two weeks and four weeks, with the nano-patterned side facing the dermis [63]. After two weeks of implantation, the ratio of Arg-1 to iNOS expression of macrophages adjacent to 55 nanometer (nm) nano-patterned BMGs (BMG-55) implants increased significantly compared to flat BMGs. Macrophage fusion with fibrous capsule thickness declined after four weeks of implantation. In addition, the vessel's number and size in tissues surrounding BMG-55 implants increased in two weeks of implantation and decreased in four weeks of implantation. The results indicated nano-patterning of BMG implants as a promising method to modulate macrophage polarization for the immune response. Surface roughness and biochemical composition of BMGs might affect biocompatibility, cell responses, and immune response.

6. Anti-Corrosion Behavior and Biocompatibility of a BMGs Implant for Biomaterial Applications

To apply the BMGs' implant for orthopaedic and dental biomaterials, anti-corrosion behavior and biocompatibility are greatly important and should be evaluated. When the implant of particular material is contact with tissues, the cell biological activity for the implant and material degradation in the body environment may occur. These could lead the constituent metal ions or implant particles to release into the body and cause reactions including allergic and toxic ones. Through *in vitro* tests and *in vivo* animal tests, Zr-based BMGs and Ti-based BMGs have been shown to have excellent anti-corrosion behavior and biocompatibility. Based on these *in vitro* tests and *in vivo* animal tests, Zr-based BMGs and Ti-based BMGs may be promising biomaterials.

7. Biomaterials for Dental Device Materials

When dealing with biomaterials for dental implants, adhesiveness of the implant surfaces to oral bacteria should be reviewed. In the oral environment, dental implants are easily accessible to microbial contamination. Key points regarding bacterial adherence is biofilm formation on biomaterial implants [64]. Biofilm formation functions to protect from antibiotics, which causes threats of infecting the biomaterial implants. Biofilm growth is controlled by physical, chemical, and biological factors. Extra polysaccharide substances control the binding and cell adhesion to the implant surface. The extra polysaccharide substances act as a barrier and protects the microbes during adverse conditions. The

biological behavior depends on the chemical composition as well as morphology of the implant surface. To improve surface properties of biomedical implants, various trials using physical and chemical techniques have been attempted. These trials aim to facilitate bio-integration and prevent bacterial adhesion. Controlling bacterial adhesion, biofilm formation, and biofilm-associated infection are essential to prevent infection surrounding dental implants.

Biofilm formation is directly influenced by electrostatic interactions between bacteria and chemical composition of the implant surface. ZrO₂ and Ti are hydrophobic materials, which attract forces and electrostatic charge interactions between bacteria and the implant surface and prevent bacterial adhesion. The influence of physical and chemical characteristics of ZrO₂ and Ti surfaces on bacterial adhesion were investigated when compared to bovine enamel simulating human oral tooth [65]. In the study, *Streptococcus mutans* (*S. mutans*) and *Porphyromonas gingivalis* (*P. gingivalis*) were used as common pathogens of the oral cavity. The results of surface hydrophobicity on bacterial adhesion indicated that ZrO₂ and Ti surfaces could prevent bacterial adhesion more than bovine enamel for both *S. mutans* and *P. gingivalis*. Accordingly, Zr-based and Ti-based BMGs are good candidates for dental device materials or implant abutment surfaces. Further *in vitro* and *in vivo* tests using Zr-based and Ti-based BMGs are needed to discuss the prevention of infection surrounding dental implants.

8. Conclusions and Prospects for the Future

A recent article showed potentials of Ti, Zr, Fe, Mg, Zn, Ca, and Sr-based BMGs in biomedical applications [66]. This article specializes in Zr-based and Ti-based BMGs, which are non-biodegradable, higher strength, higher elasticity, higher failure resistance, and lower Young's modulus compared with crystalline alloys. This article also refers to dental applications including adhesiveness of material surfaces to oral bacteria. BMGs have great potentials in biomedical applications especially as orthopaedic and dental device materials. Zr-based BMGs and Ti-based BMGs have both excellent mechanical properties and corrosion resistance. Those BMGs can be used as orthopaedic and dental device materials, such as implanted pins, screws, plates, nails, and dental implants. They can also be used as minimally invasive surgical devices. Orthopaedic and dental device materials are needed to survive in a harsh human body environment for a long time. Anti-corrosion behavior and biocompatibility of Zr-based BMGs and a Ti-based BMGs implant have been proven through *in vitro* tests and *in vivo* animal tests.

One of the problems of the current BMGs, the limited diameter sizes restrain the design and types of biomedical devices using BMGs. One promising measure to solve the limited components size of BMGs is a thin film form of Zr-based and Ti-based BMGs. Metallic glass coating using thin film form onto the substrate of biomedical devices might widen the design and types of implants. A thin film form of Zr-based and Ti-based BMGs can exhibit a combination of large mechanical properties with good biocompatibility [67] and cytocompatibility [68]. In addition, a thin film form of Zr-based BMGs showed size effects on mechanical properties, which can be used as coatings for biomedical applications [69,70]. In addition, future technology might overcome the size limitation. When BMGs with larger sizes are obtained, further *in vivo* animal tests of BMGs pins, screws, plates, nails, and dental implants can be proceeded, which may lead to clinical application as orthopaedic and dental device materials.

The other problem of BMGs is the localization of deformation within shear bands reporting a brittle-like failure behavior. This limitation is extremely important especially for *in vivo* applications, which directly connects with clinical application as orthopaedic and dental device materials. This mechanical property of BMGs could restrain the clinical application. To coat a metallic glass with a thin film form of BMGs onto the substrate of biomedical devices might solve this problem. For future work in this field, metallic glass coating techniques with a thin film form of BMGs including *in vitro* and *in vivo* studies are recommended.

Author Contributions: K.I. designed the study. K.I. and X.Z. contributed to data acquisition. K.I. drafted the manuscript. X.Z. checked and revised the manuscript. X.L. contributed to the English proofreading. All authors have read and agreed to the published version of the manuscript.

Funding: This research received no external funding.

Acknowledgments: The authors are grateful to Takao Hanawa, Sachiko Hiromoto and Isao Ohnishi for valuable discussions.

Conflicts of Interest: The authors declare no conflict of interest.

References

1. Antunes, R.A.; de Oliveira, M.C. Corrosion processes of physical vapor deposition-coated metallic implants. *Crit. Rev. Biomed. Eng.* **2009**, *37*, 425–460. [[CrossRef](#)] [[PubMed](#)]
2. Whitaker, R.A. Environmental effects on the life of bone-plate-type surgical implants. *Rev. Environ. Health* **1982**, *4*, 63–82.
3. Molster, A.O. Biomechanical effects of intramedullary reaming and nailing on intact femora in rats. *Clin. Orthop.* **1986**, *202*, 278–285.
4. Bradley, G.W.; McKenna, G.B.; Dunn, H.K.; Daniels, A.U.; Statton, W.O. Effects of flexural rigidity of plates on bone healing. *J. Bone Joint Surg. Am.* **1979**, *61*, 866–872. [[CrossRef](#)] [[PubMed](#)]
5. Woo, S.L.; Akeson, W.H.; Coutts, R.D.; Rutherford, L.; Doty, D.; Jemmott, G.F.; Amiel, D. A comparison of cortical bone atrophy secondary to fixation with plates with large differences in bending stiffness. *J. Bone Joint Surg. Am.* **1976**, *58*, 190–195. [[CrossRef](#)] [[PubMed](#)]
6. Tonino, A.J.; Davidson, C.L.; Klopper, P.J.; Linclau, L.A. Protection from stress in bone and its effects. Experiments with stainless steel and plastic plates in dogs. *J. Bone Joint Surg. Br.* **1976**, *58*, 107–113. [[CrossRef](#)]
7. Uhthoff, H.K.; Dubuc, F.L. Bone structure changes in the dog under rigid internal fixation. *Clin. Orthop.* **1971**, *81*, 165–170. [[CrossRef](#)]
8. Inoue, A. Stabilization of supercooled liquid and opening-up of bulk glassy alloys. *Proc. Jpn. Acad. Ser. B* **1997**, *73*, 19–24. [[CrossRef](#)]
9. Inoue, A.; Zhang, T. Fabrication of Bulk Glassy $Zr_{55}Al_{10}Ni_5Cu_{30}$ Alloy of 30 mm in Diameter by a Suction Casting Method. *Mater. Trans.* **1996**, *37*, 185–187. [[CrossRef](#)]
10. Inoue, A.; Nishiyama, N.; Kimura, H. Preparation and thermal stability of bulk amorphous $Pd_{40}Cu_{30}Ni_{10}P_{20}$ alloy cylinder of 72 mm in diameter. *Mater. Trans.* **1997**, *38*, 179–183. [[CrossRef](#)]
11. Zhang, W.; Inoue, A. Formation and mechanical strength of new Cu-based bulk glassy alloys with large supercooled liquid region. *Mater. Trans.* **2004**, *45*, 1210–1213. [[CrossRef](#)]
12. Schroers, J.; Johnson, W.L. Highly processable bulk metallic glass-forming alloys in the Pt–Co–Ni–Cu–P system. *Appl. Phys. Lett.* **2004**, *84*, 3666–3668. [[CrossRef](#)]
13. Zheng, Q.; Xu, J.; Ma, E. High glass-forming ability correlated with fragility of Mg–Cu(Ag)–Gd alloys. *J. Appl. Phys.* **2007**, *102*, 113519-1–113519-5. [[CrossRef](#)]
14. Li, R.; Pang, S.; Ma, C.; Zhang, T. Influence of similar atom substitution on glass formation in (La–Ce)–Al–Co bulk metallic glasses. *Acta Mater.* **2007**, *55*, 3719–3726. [[CrossRef](#)]
15. Yokoyama, Y.; Mund, E.; Inoue, A.; Schultz, L. Production of $Zr_{55}Cu_{30}Ni_5Al_{10}$ glassy alloy rod of 30 mm in diameter by a cap-cast technique. *Mater. Trans.* **2007**, *48*, 3190–3192. [[CrossRef](#)]
16. Zeng, Y.; Nishiyama, N.; Yamamoto, T.; Inoue, A. Ni-Rich bulk metallic glasses with high glass-forming ability and good metallic properties. *Mater. Trans.* **2009**, *50*, 2441–2445. [[CrossRef](#)]
17. Takeuchi, A.; Inoue, A. Classification of bulk metallic glasses by atomic size difference, heat of mixing and period of constituent elements and its application to characterization of the main alloying element. *Mater. Trans.* **2005**, *46*, 2817–2829. [[CrossRef](#)]
18. Inoue, A.; Zhang, T.; Masumoto, T. Preparation of bulky amorphous Zr–Al–Ni–Cu alloys by copper mold casting and their thermal and mechanical properties. *Mater. Trans. JIM* **1995**, *36*, 391–398. [[CrossRef](#)]
19. Wang, W.H. Roles of minor additions in formation and properties of bulk metallic glasses. *Prog. Mater. Sci.* **2007**, *52*, 540–596. [[CrossRef](#)]
20. Gilbert, C.J.; Ritchie, R.O.; Johnson, W.L. Fracture toughness and fatigue-crack propagation in a Zr–Ti–Ni–Cu–Be bulk metallic glass. *Appl. Phys. Lett.* **1997**, *71*, 476–478. [[CrossRef](#)]

21. Pang, S.J.; Zhang, T.; Kimura, H.; Asami, K.; Inoue, A. Corrosion behavior of Zr-(Nb)-Al-Ni-Cu glassy alloys. *Mater. Trans. JIM* **2000**, *41*, 1490–1494. [[CrossRef](#)]
22. Wang, J.G.; Choi, B.M.; Nieh, T.G.; Liu, C.T. Nano-scratch behavior of a bulk Zr-10Al-5Ti-17.9Cu-14.6Ni amorphous alloy. *J. Mater. Res.* **2000**, *15*, 913–922. [[CrossRef](#)]
23. Liu, L.; Qiu, C.L.; Zou, H.; Chan, K.C. The effect of the microalloying of Hf on the corrosion behavior of ZrCuNiAl bulk metallic glass. *J. Alloys Compd.* **2005**, *399*, 144–148. [[CrossRef](#)]
24. Boyer, R.; Welsch, G.; Collings, E.W. Titanium Alloys. In *Materials Properties Handbook*; ASM International: Materials Park, OH, USA, 1994.
25. Hanawa, T.; Yoneyama, T. Metals. In *Biomaterials*; Corona Publishing CO., LTD.: Tokyo, Japan, 2007.
26. Long, M.; Rack, H.J. Titanium alloys in total joint replacement—A materials science perspective. *Biomaterials* **1998**, *19*, 1621–1639. [[CrossRef](#)]
27. Niinomi, M. Mechanical properties of biomedical titanium alloys. *Mater. Sci. Eng. A* **1998**, *243*, 231–236. [[CrossRef](#)]
28. Katsamanis, F.; Raftopoulos, D.D. Determination of mechanical properties of human femoral cortical bone by the Hopkinson bar stress technique. *J. Biomech.* **1990**, *23*, 1173–1184. [[CrossRef](#)]
29. Choi, K.; Kuhn, J.L.; Ciarelli, M.J.; Goldstein, S.A. The elastic moduli of human subchondral, trabecular, and cortical bone tissue and the size-dependency of cortical bone modulus. *J. Biomech.* **1990**, *23*, 1103–1113. [[CrossRef](#)]
30. Kopperdahl, D.L.; Keaveny, T.M. Yield strain behavior of trabecular bone. *J. Biomech.* **1998**, *31*, 601–608. [[CrossRef](#)]
31. Turner, C.H.; Wang, T.; Burr, D.B. Shear strength and fatigue properties of human cortical bone determined from pure shear tests. *Calcif. Tissue Int.* **2001**, *69*, 373–378. [[CrossRef](#)]
32. Wang, G.Y.; Liaw, P.K.; Yokoyama, Y.; Inoue, A.; Liu, C.T. Fatigue behavior of Zr-based bulk-metallic glasses. *Mater. Sci. Eng. A* **2008**, *494*, 314–323. [[CrossRef](#)]
33. Maruyama, N.; Nakazawa, K.; Hanawa, T. Fatigue properties of Zr-based amorphous alloy in phosphate buffered saline solution. *Mater. Trans.* **2002**, *43*, 3118–3121. [[CrossRef](#)]
34. Wang, G.; Liaw, P.K.; Yokoyama, Y.; Freels, M.; Inoue, A. Investigations of the factors that affected fatigue behavior of Zr-based bulk-metallic glasses. *Adv. Eng. Mater.* **2008**, *10*, 1030–1033. [[CrossRef](#)]
35. Liu, L.; Qiu, C.L.; Chen, Q.; Chan, K.C.; Zhang, S.M. Deformation behavior, corrosion resistance, and cytotoxicity of Ni-free Zr-based bulk metallic glasses. *J. Biomed. Mater. Res. Part A* **2008**, *86*, 160–169. [[CrossRef](#)] [[PubMed](#)]
36. Huang, L.; Yokoyama, Y.; Wu, W.; Liaw, P.K.; Pang, S.; Inoue, A.; Zhang, T.; He, W. Ni-free Zr-Cu-Al-Nb-Pd bulk metallic glasses with different Zr/Cu ratios for biomedical applications. *J. Biomed. Mater. Res. Part B Appl. Biomater.* **2012**, *100*, 1472–1482. [[CrossRef](#)] [[PubMed](#)]
37. Liu, Y.; Wang, Y.M.; Pang, H.F.; Zhao, Q.; Liu, L. A Ni-free ZrCuFeAlAg bulk metallic glass with potential for biomedical applications. *Acta Biomater.* **2013**, *9*, 7043–7053. [[CrossRef](#)]
38. Inoue, A.; Wang, X.M.; Zhang, W. Developments and applications of bulk metallic glasses. *Rev. Adv. Mater. Sci.* **2008**, *18*, 1–9.
39. Hiromoto, S.; Tsai, A.-P.; Sumita, M.; Hanawa, T. Effect of chloride ion on the polarization behavior of the Zr₆₅Al_{7.5}Ni₁₀Cu_{17.5} amorphous alloy in phosphate buffered solution. *Corr. Sci.* **2000**, *42*, 1651–1660. [[CrossRef](#)]
40. Hiromoto, S.; Tsai, A.-P.; Sumita, M.; Hanawa, T. Effect of surface finishing and dissolved oxygen on the polarization behavior of Zr₆₅Al_{7.5}Ni₁₀Cu_{17.5} amorphous alloy in phosphate buffered solution. *Corr. Sci.* **2000**, *42*, 2167–2185. [[CrossRef](#)]
41. Hiromoto, S.; Tsai, A.-P.; Sumita, M.; Hanawa, T. Effect of pH on the polarization behavior of Zr₆₅Al_{7.5}Ni₁₀Cu_{17.5} amorphous alloy in a phosphate-buffered solution. *Corr. Sci.* **2000**, *42*, 2193–2200. [[CrossRef](#)]
42. Hiromoto, S.; Asami, K.; Tsai, A.-P.; Sumita, M.; Hanawa, T. Surface composition and anodic polarization behavior of zirconium-based amorphous alloy with various alloying elements in a phosphate buffered saline solution. *J. Electrochem. Soc.* **2002**, *149*, B117–B122. [[CrossRef](#)]
43. Hiromoto, S.; Hanawa, T. Re-passivation current of amorphous Zr₆₅Al_{7.5}Ni₁₀Cu_{17.5} alloy in a Hanks' balanced solution. *Electrochim. Acta* **2002**, *47*, 1343–1349. [[CrossRef](#)]

44. Hiromoto, S.; Tsai, A.-P.; Sumita, M.; Hanawa, T. Surface characterization of Zr-Al-(Ni, Cu) amorphous alloys immersed in a cell-culture medium. *Mater. Trans. JIM* **2002**, *43*, 261–266. [[CrossRef](#)]
45. Morrison, M.L.; Buchanan, R.A.; Leon, R.V.; Liu, C.T.; Green, B.A.; Liaw, P.K.; Horton, J.A. The electrochemical evaluation of a Zr-based bulk metallic glass in a phosphate-buffered saline electrolyte. *J. Biomed. Mater. Res. Part A* **2005**, *74*, 430–438. [[CrossRef](#)] [[PubMed](#)]
46. Stansbury, E.E.; Buchanan, R.A. Faraday's Law. In *Fundamentals of Electrochemical Corrosion*; ASM International: Materials Park, OH, USA, 2000; pp. 147–149.
47. Wang, Y.B.; Zheng, Y.F.; Wei, S.C.; Li, M. In vitro study on Zr-based bulk metallic glasses as potential biomaterials. *J. Biomed. Mater. Res. Part B* **2011**, *96*, 34–46. [[CrossRef](#)] [[PubMed](#)]
48. Wataha, J.C.; Lockwood, P.E.; Schedle, A. Effect of silver, copper, mercury, and nickel ions on cellular proliferation during extended, low-dose exposures. *J. Biomed. Mater. Res.* **2000**, *52*, 360–364. [[CrossRef](#)]
49. Liu, L.; Qiu, C.L.; Huang, C.Y.; Yu, Y.; Huang, H.; Zhang, S.M. Biocompatibility of Ni-free Zr-based bulk metallic glasses. *Intermetallics* **2009**, *17*, 235–240. [[CrossRef](#)]
50. Monfared, A.; Vali, H.; Faghihi, S. Biocorrosion and biocompatibility of Zr–Cu–Fe–Al bulk metallic glasses. *Surf. Interface Anal.* **2013**, *45*, 1714–1720. [[CrossRef](#)]
51. Li, J.; Shi, L.L.; Zhu, Z.D.; He, Q.; Ai, H.J.; Xu, J. Zr₆₁Ti₂Cu₂₅Al₁₂ metallic glass for potential use in dental implants; Biocompatibility assessment by in vitro cellular responses. *Mater. Sci. Eng. C* **2013**, *33*, 2113–2121. [[CrossRef](#)]
52. Fornell, J.; Van Steenberge, N.; Varea, A.; Rossinyol, E.; Pellicer, E.; Suriñach, S.; Baró, M.D.; Sort, J. Enhanced mechanical properties and in vitro corrosion behavior of amorphous and devitrified Ti₄₀Zr₁₀Cu₃₈Pd₁₂ metallic glass. *J. Mech. Behav. Biomed. Mater.* **2011**, *4*, 1709–1717. [[CrossRef](#)]
53. Blanquer, A.; Pellicer, E.; Hynowska, A.; Barrios, L.; Ibáñez, E.; Baró, M.D.; Sort, J.; Nogués, C. In vitro biocompatibility assessment of Ti₄₀Cu₃₈Zr₁₀Pd₁₂ bulk metallic glass. *J. Mater. Sci. Mater. Med.* **2014**, *25*, 163–172. [[CrossRef](#)]
54. Wang, Y.B.; Li, H.F.; Cheng, Y.; Zheng, Y.F.; Ruan, L.Q. In vitro and in vivo studies on Ti-based bulk metallic glass as potential dental implant material. *Mater. Sci. Eng. C* **2013**, *33*, 3489–3497. [[CrossRef](#)] [[PubMed](#)]
55. Imai, K.; Hiromoto, S. In vivo evaluation of Zr-based bulk metallic glass alloy intramedullary nails in rat femora. *J. Mater. Sci. Mater. Med.* **2014**, *25*, 759–768. [[CrossRef](#)] [[PubMed](#)]
56. Sun, Y.; Huang, Y.; Fan, H.; Wang, Y.; Ning, Z.; Liu, F.; Feng, D.; Jin, X.; Shen, J.; Sun, J.; et al. In vitro and in vivo biocompatibility of an Ag-bearing Zr-based bulk metallic glass for potential medical use. *J. Non-Cryst. Solids* **2015**, *419*, 82–91. [[CrossRef](#)]
57. Imai, K.; Hiromoto, S. In vivo evaluation of bulk metallic glasses for osteosynthesis devices. *Materials* **2016**, *9*, 676. [[CrossRef](#)] [[PubMed](#)]
58. Imai, K. In vivo investigation of Zr-based bulk metallic glasses sub-periosteally implanted on the bone surface. *J. Mater. Sci. Chem. Eng.* **2016**, *4*, 46–51. [[CrossRef](#)]
59. Kokubun, R.; Wang, W.; Zhu, S.; Xie, G.; Ichinose, S.; Itoh, S.; Takakuda, K. In vivo evaluation of a Ti-based bulk metallic glass alloy bar. *Bio-Med. Mater. Eng.* **2015**, *26*, 9–17. [[CrossRef](#)]
60. Lin, C.H.; Chen, C.H.; Huang, Y.S.; Huang, C.H.; Huang, J.C.; Jang, J.S.C.; Lin, Y.S. In-vivo investigations and cytotoxicity tests on Ti/Zr-based metallic glasses with various Cu contents. *Mater. Sci. Eng. C* **2017**, *77*, 308–317. [[CrossRef](#)]
61. Wong, C.C.; Wong, P.C.; Tsai, P.H.; Jang, J.S.; Cheng, C.K.; Chen, H.H.; Chen, C.H. Biocompatibility and osteogenic capacity of Mg-Zn-Ca bulk metallic glass for rabbit tendon-bone interference fixation. *Int. J. Mol. Sci.* **2019**, *20*, 2191. [[CrossRef](#)]
62. Basu, B.; Sabareeswaran, A.; Shenoy, S.J. Biocompatibility property of 100% strontium-substituted SiO₂-Al₂O₃-P₂O₅-CaO-CaF₂ glass ceramics over 26 weeks implantation in rabbit model: Histology and micro-Computed Tomography analysis. *J. Biomed. Mater. Res. Part B Appl. Biomater.* **2015**, *103*, 1168–1179. [[CrossRef](#)]
63. Shayan, M.; Padmanabhan, J.; Morris, A.H.; Cheung, B.; Smith, R.; Schroers, J.; Kyriakides, T.R. Nanopatterned bulk metallic glass-based biomaterials modulate macrophage polarization. *Acta Biomater.* **2018**, *75*, 427–438. [[CrossRef](#)]
64. Veerachamy, S.; Yarlagadda, T.; Manivasagam, G.; Yarlagadda, P.K. Bacterial adherence and biofilm formation on medical implants: A review. *Proc. Inst. Mech. Eng. Part H* **2014**, *228*, 1083–1099. [[CrossRef](#)] [[PubMed](#)]

65. Avila, E.D.; Molon, R.S.; Lima, B.P.; Lux, R.; Shi, W.; Junior, M.J.; Spolidorio, D.M.; Vergani, C.E.; Assis Mollo Junior, F. Impact of physical chemical characteristics of abutment implant surfaces on bacteria adhesion. *J. Oral Implantol.* **2016**, *42*, 153–158. [[CrossRef](#)] [[PubMed](#)]
66. Li, H.F.; Zheng, Y.F. Recent advances in bulk metallic glasses for biomedical applications. *Acta Biomater.* **2016**, *36*, 1–20. [[CrossRef](#)] [[PubMed](#)]
67. Subramanian, B.; Maruthamuthu, S.; Rajan, S.T. Biocompatibility evaluation of sputtered zirconium-based thin film metallic glass-coated steels. *Int. J. Nanomed.* **2015**, *10*, 17–29. [[CrossRef](#)] [[PubMed](#)]
68. Thanka, R.S.; Bendavid, A.; Subramanian, B. Cytocompatibility assessment of Ti-Nb-Zr-Si thin film metallic glasses with enhanced osteoblast differentiation for biomedical applications. *Colloids Surf. B Biointerfaces* **2019**, *173*, 109–120. [[CrossRef](#)] [[PubMed](#)]
69. Ghidelli, M.; Gravier, S.; Blandin, J.J.; Djemia, P.; Momprou, F.; Abadias, G.; Raskin, J.P.; Pardoen, T. Extrinsic mechanical size effects in thin ZrNi metallic glass films. *Acta Mater.* **2015**, *90*, 232–241. [[CrossRef](#)]
70. Ghidelli, M.; Idrissi, H.; Gravier, S.; Blandin, J.J.; Raskin, J.P.; Schryvers, D.; Pardoen, T. Homogeneous flow and size dependent mechanical behavior in highly ductile Zr₆₅Ni₃₅ metallic glass films. *Acta Mater.* **2017**, *131*, 246–259. [[CrossRef](#)]



© 2020 by the authors. Licensee MDPI, Basel, Switzerland. This article is an open access article distributed under the terms and conditions of the Creative Commons Attribution (CC BY) license (<http://creativecommons.org/licenses/by/4.0/>).